An Approach for the Direct Inclusion of Weather Information in the Power Flow

Thomas J. Overbye, Texas A&M University, overbye@tamu.edu
Farnaz Safdarian, Texas A&M University, fsafdarian@tamu.edu
Wei Trinh, Texas A&M University, weit1@tamu.edu
Zeyu Mao, Texas A&M University, zeyumao2@tamu.edu
Jonathan Snodgrass, Texas A&M University, snodgrass@tamu.edu
Juhee Yeo, Texas A&M University, yeochee26@tamu.edu

Abstract

While it is widely recognized that weather impacts the power flow, historically weather information has only been implicitly included. This paper presents an approach for the direct inclusion of weather information in the power flow. Key issues addressed by the paper include the availability of weather information, the mapping of weather information to electric grid components, a flexible and extensible modeling approach for relating weather values to the power flow models, and the visualization of the weather impacts. The approach is demonstrated on several electric grids ranging in size from 7000 to 82,000 buses using weather data over several different years.

Keywords: power flow, weather, electric grid modeling, visualization

1. Introduction

The power flow and related applications such as the optimal power flow (OPF) are some of the most common tools used to study and design large-scale, high voltage electric grids. As is common to all engineering analysis tools, there are tradeoffs associated with the amount of details included in the electric grid models that are used in the power flow. Factors associated with these tradeoffs include the existence of the models themselves, the availability of the model parameter information, the memory required to store the parameters, the computational complexity required to utilize the model, and the ultimate impact of the models on the results. The purpose of this paper is to show that relatively detailed weather information, including insolation, can become a normal part of the standard power flow.

Before getting into the specifics, it is helpful to briefly consider what is, and what isn't, currently included in the large-scale power flow models that are the focus of this paper. When the digital power flow was first introduced in the late 1950's and early 1960's [1], [2] the goal was to solve as large of systems as possible with memory being a key constraint ([2] notes the solution of grids with up to 1000 buses using just 32 KB of memory). Hence transmission-level power flows started out just modeling positive sequence models. An early 1970's description of the core power flow models is given in [3] with a more recent description of standardized power flow models and parameters given in [4] and [5].

In comparing [3], written when computer memory was still very much a constraint, with these more recent power flow model descriptions, qualitatively the changes have been relatively modest. Certainly there are now more parameters, including the modeling of device limits, and there are now objects for individual generators, loads, three-winding transformers, and HVDC lines. There are also a few new types of models, such as the representation of transformer impedance correction tables [6], generator reactive capability curves, and device ownership.

An example of something that has not changed is that the positive sequence power flow, with its assumptions of a perfectly balanced three-phase grid and uniformly transposed transmission lines. This approach continues to be used almost exclusively for transmission system power flow analysis even though the benefits of the three-phase power flow are well known [7]. This is a case in which the computation and model simplicity benefits of the positive sequence approach are seen as outweighing the benefits, but much higher modeling requirements, of the three-phase approach. An example of a modeling change that has occurred is the now widespread use of the DC power flow [8] particularly for electric market analysis. While the DC power flow is certainly less accurate, its much simpler linear computation and fewer data requirements make it a very attractive choice for at least some applications.

Sitting between these two modeling examples is the paper's focus on normalizing the explicit inclusion of weather information in the power flow. Of course, since electric grids have long been significantly impacted by weather, its impact has usually been implicitly included. This includes the modeled load values, assumed values for generator real power output limits, transmission line and transformer limits, and

URI: https://hdl.handle.net/10125/102961
978-0-9981331-6-4

even the resistance values for these devices. While this approach has historically usually been adequate, a number of different recent changes are making it such that the advantages of direct inclusion of weather now appear to outweigh the disadvantages. Certainly one problem with the implicit approach is when modeling assumptions are not explicit, such as when temperatures fall outside assumed ranges, grid problems can occur, such as was the case in February 2021 in Texas during Winter Storm Uri [9]. The need for better weather inclusion is also noted in [10], [11].

The remainder of the paper is organized as follows. Section 2 addresses the issues needed to effectively include weather directly into the power flow. Then Section 3 introduces the electric grids and weather sets that will be used for the examples throughout the remainder of the paper. The following section provides some specific examples, while Section 5 provides some future directions.

2. Considerations for Weather Inclusion in the Power Flow

In order to explicitly include weather information in a power flow model there is a need to 1) have adequate weather information for the electric grid footprint of interest, 2) be able to map the weather information to pertinent electric grid components, and 3) have adequate models of how the weather impacts the grid components. This section addresses each of these objectives.

With respect to the availability of past and present weather information, it is safe to say that it is widely available. As an example, for the research related to this paper the team obtained hourly historical weather data for many sites worldwide covering a date range from the 1940's to 2022 [12]. While the number of weather stations has increased over the years, even in the late 1940's data is available for about 600 stations in the contiguous USA. Figure 1 shows these stations, along with a contour of the temperature from January 31, 1949 when the low temperatures in some parts of Texas were significantly below those seen during Uri; later in the paper this weather will be applied to modern grids.

Concerning the weather stations to use, as a minimum there should be coverage over the electrical footprint of interest. There is no single standard for identifying weather stations, but the International Civil Aviation Organization (ICAO) provides data for more than 22,000 locations worldwide using 4-letter identifiers, with each location having a specified latitude, longitude and elevation. As an example, real-time weather information for about 5000 stations using the ICAO identifiers is available at [13]. The World Meteorological Organization (WMO) uses five digit identifiers. For electric grid studies these stations could be supplemented with information from weather monitoring sites maintained by the electric utilities. The types of measurements needed would be modest, with the approach presented here using temperature, wind speed and cloud cover percentage (the data sets also had dew point and wind direction, but they were not used here). For the results presented here, the measurement times are given using Coordinated Universal Time (UTC) in the ISO8601 format. For solar PV the insolation is estimated by using the time, latitude and longitude to determine the sun's azimuth and elevation, and then combining this with the cloud cover percentage.

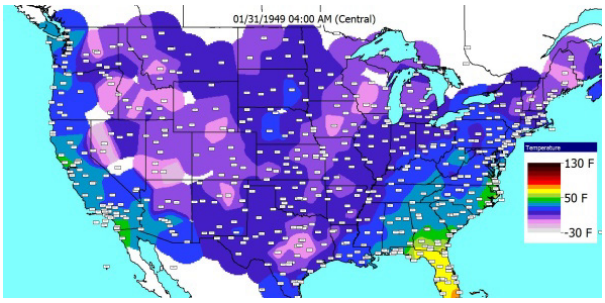

Figure 1: Temperature Contour for January 31, 1949

Given that power flows sometimes study grids many years in the future, these situations also need to be considered. One approach would be for the Electric Reliability Organizations (EROs) to select a set of times from the past that represent the desired conditions. Examples could include a hot summer day with high winds, a similar day without much wind, a fall night, etc. A complementary approach would be for the EROs (working with their meteorological staff) to develop or obtain a set of hypothesized future weather conditions, noting that there are many different entities who create such models. Whether the data is historic or forecasted, an advantage of including the weather with the power flow case is the underlying assumed weather is then explicit.

The second objective is to map the weather information to the electric grid components. Traditionally power flow data sets have not included geographic information for the electric substations. However, this is rapidly changing driven in part by 1) the widespread availability of geographic information systems, 2) visualization techniques that can leverage geographic information [14], and 3) the need for geographic information for geomagnetic disturbance studies [15]. Examples of NERC regions requiring the submission of geographic information include [5], [16], and [17]. Large-scale synthetic electric grids with electric substation latitudes and longitudes are also

available [18], [19], [20]. Finally, in the US the latitudes and longitudes for all generators larger than 1 MW are available at [21]. Hence most present day power flow models already either directly have the needed geographic information, or have it in supplemental files.

To integrate weather into power flow analysis what is needed is to have such information at the locations of the grid components such as the generators and transmission lines. Given the now widespread availability of weather stations, weather information is usually available at least close by to the electric grid location. Then 2D scattered data interpolation methods can be used to provide good estimates of values at the desired grid locations. While there is no best method for all situations, Delaunay triangulation or using the closest station with valid measurements works well in most situations. As an example Figure 2 shows a contour of the temperatures during Winter Storm Uri in 2021 using data from more than 2500 stations. When using this data with the 110,000 bus and 43,000 electric substations of the actual North American power grid used in [22], the average distance between an electric substation and the closest weather station is 19.8 km.

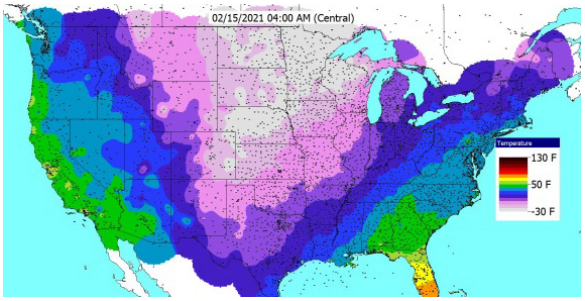

Figure 2: Temperature Contour for February 15, 2021

However, there certainly can be situations in which standard interpolation does not work well, such as mountains, valleys and some coastal regions. For these the approach utilized here is to use data from a specified weather station regardless of distance. A specific example is the Columbia River Gorge, which divides the US states of Washington and Oregon. With a length of about 190 km and average width of 5 km, the gorge has a unique and complex climate that can include quite high winds [23]. This has resulted in the siting of a large amount of wind generation, with the characteristic that the wind speeds at the wind power plants (WPPs) in the gorge can be quite different from nearby weather stations outside the gorge. Figure 3 visualizes the generation (from the 82,000-bus grid introduced in the next section) and weather stations in the gorge using the geographic data view (GDV) approach from [14] in which the ovals show the generation capacity with the colors indicating the fuel type (green for wind, blue for hydro, black for coal, red for nuclear, brown for natural gas, and yellow for solar); the white rectangles show the weather stations.

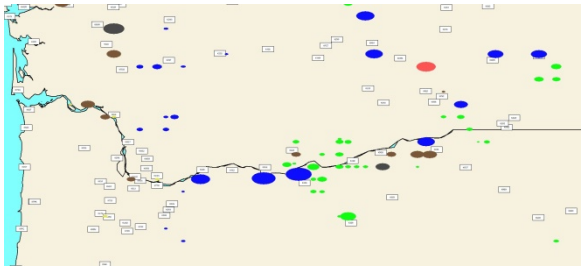

Figure 3: Generators and Weather Stations in the Columbia River Gorge

The last objective is having adequate models of how the weather impacts the various grid components. What is proposed here is to mimic the multi-model approach widely used in electric grid stability analysis. In this stability method a number of different model types are available to represent different system components. The set of available models for the different components started small [24] with an initial focus on just the synchronous generators, and then gradually expanded and became more standardized. As an example, [25] and [26] illustrate the change in generator exciter modeling. Now it is common for stability software vendors to support 100's of different models covering a gradually expanded set of electric grid object classes (e.g., synchronous generators, renewable generators, loads, HVDC lines, relays, etc.) based upon the needs of their customers. In a similar manner the initial set of supported weather models would start small and grow as needs changed.

The purpose of this paper is to present and demonstrate an overall methodology on large-scale grids. The paper's purpose is not to introduce any new models since there are already a wide number available in the literature covering the impact of weather on many different power flow models. Examples include generator maximum MW output, transmission line ambient-adjusted ratings [27], dynamic transmission line ratings [28], and temperature dependent transmission line resistance [29]. Rather here just six somewhat generic models are used, with all modeling the impact of various weather values on the maximum real power output values for electric generators. The assumption, well supported by available data, is that the geographic location of each generator is known.

The first model provides a simple representation for the WPP real power output, taking the local wind speed as an input. This model utilizes the wind turbine power curve models of [30], [31], and [32]. Parameters include the rated real power (MW), the cut-

in wind speed, the rated wind speed, the cut-out wind speed, and a scalar multiplier to estimate the hub height winds from surface winds. The second to fourth models are similar to the first, except that they provide somewhat generic power curve representations of the three IEC wind turbine classes using data from [33]. The Section 4 discusses the sensitivity of the results to these different models with Figure 17 showing the four speed-power curves.

The fifth model represents solar PV power generation, taking the local cloud cover percentage and the date/time as inputs, and providing the maximum real power as the output, implementing the models of [30]. Parameters include the rated real power, the type of solar PV tracking (fixed, single-axis, dual-axis), the azimuth, the tilt angle, and an assumed sky diffuse factor. For wind and solar generators in the USA, many of these parameters are available in [21].

The sixth model provides a simple approximation of how generator real power output limits vary with temperature, taking temperature as an input and providing a scalar on the maximum real power value as an output. The parameters for this model are shown in Figure 4, with the right side modeling the well-known reduction in output (for at least gas turbines) with increasing ambient temperature [34]. The left side models the reduction in output with decreasing temperature, with the assumption that this model is more intended to represent the potential for generators to fail rather than describing an explicit temperature dependence. The increasing likelihood of generator failures with cold temperatures is described in [9] and [35]. Either the left or right side can be omitted just by setting the corresponding scale value to 1.0.

3. Example Electric Grids and Weather Data

In order to show that weather can become a normal part of standard power flow analysis, this paper utilizes five geographically-based, larger-scale electric grids. The first four are synthetic grids [36] whereas the last is the previously mentioned 110,000-bus grid modeling a proposed interconnection of the North American Eastern and Western grids [22]. The oneline for the first synthetic grid, which has 6700 buses and covers a geographic footprint of most of the US state of Texas, is shown in Figure 5. The grid's nominal voltage levels are 345 kV (red), 138 kV (black) and 69 kV (gray). The grid has a total of about 105 GW of generation, with 25 GW of wind and 2.3 GW of solar. Figure 6 shows the grid's generation capacity using the same GDV approach as used in Figure 3; the size and location of the generation is based on 2019 EIA 860 data. The second grid is similar to the first except the amount of solar and wind generation capacity has been increased to what could occur in 2030 (assuming extremely high renewable growth). It has a total of about 55 GW of wind and 27 GW of solar (for reference in 2022 Texas has a total of about 46 GW of wind and solar).

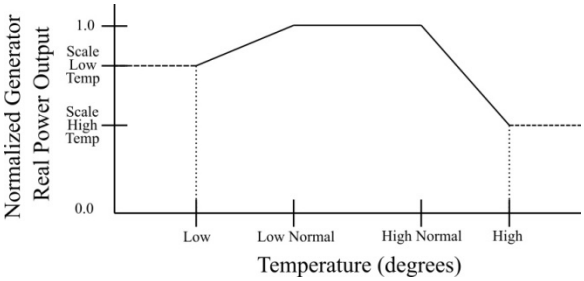

Figure 4: Piecewise Linear Temperature Model

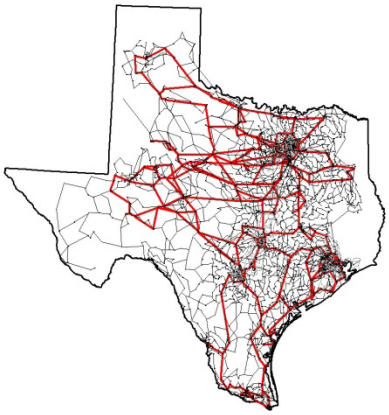

Figure 5: 6700 Bus Grid Oneline

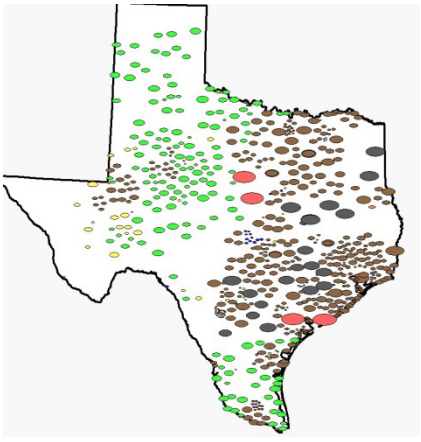

Figure 6: 6700 Bus Grid Generation GDV

The third synthetic grid has about 24,000 buses and 6300 generators with a total of 320 GW of generation including 47 GW of wind and 1.8 GW of solar. Its oneline is shown in Figure 8 using the same nominal voltage color convention with additional

voltage levels of 500 kV (orange) and 230 kV (blue). The size and location of its generators is also based on 2019 EIA 860 data. The last synthetic grid has 82,000 buses covering the contiguous US and is identical to the grid used in [22] in which 80,000 buses are used to model a combined East-West grid and 2000 buses model a separate grid covering most of Texas. The grid's oneline is shown in Figure 9 using the previous nominal voltage color convention with the addition of light green for 765 kV; the thick black line indicates the division between the East and Texas portion of the grid and the West. The power flow models for all of the synthetic grids are available at [37].

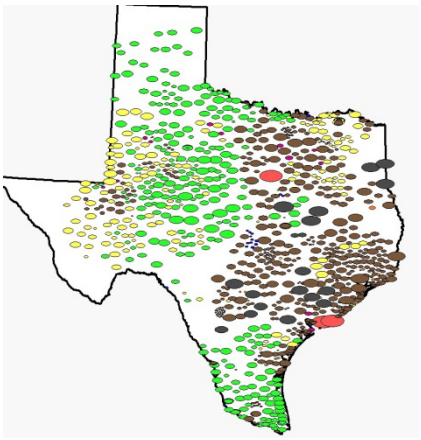

Figure 7: 6700 Bus Grid Generation GDV (2030)

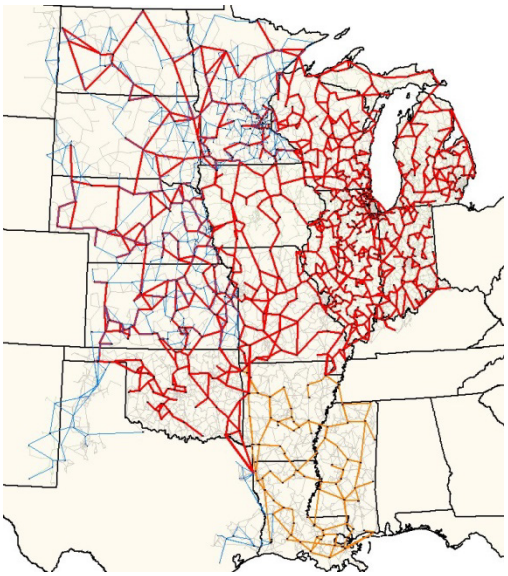

Figure 8: 24,000 Bus Online

The examples in the next section are all based on hourly historic weather data obtained from [12] dating back to the 1940's. While the source contains worldwide data, for this paper the examples are restricted to North American measurements. The number of weather stations with valid measurements varies, with a general increase from about 600 in the late 1940's to 2500 in 2020. The measurements used here are 1) temperature, 2) surface wind speed, and 3) percentage cloud cover.

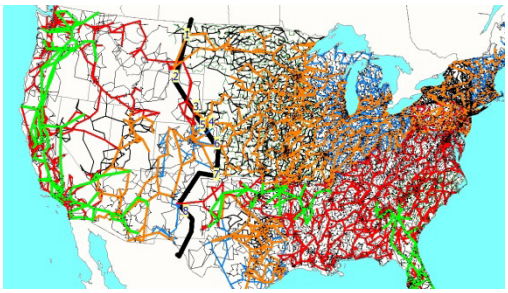

Figure 9: 82,000 Bus Grid Oneline

4. Large-Scale Grid Examples

There are many different ways weather information can be used in power flow analysis. This section provides some specific examples, within the paper's focus, of using weather to modify the output of either WPPs based on wind speed, solar PV based on insolation, and potentially all generators based on temperature. Hence these examples address the growing power flow challenge of providing coherent generator maximum power limits as the number of WPPs and solar rapidly grows.

In general, the inclusion of these examples in the power flow and/or optimal power flow is fairly straightforward. Results presented here are modeled using PowerWorld Simulator Version 23 in which during the solution process the previously described weather-dependent models are used to change the generators' maximum real power outputs limits. Additionally, since wind and solar generators often operate at their maximum, weather dependent limits, the models can change the generators' modeled real power output and potentially their on/off status. Examples in which it would usually be appropriate to directly change the generators' on/off status and power output would be wind or solar generators in the power flow which, given these generators' low costs, would typically be operating at their maximum, or would be off. Then during the power flow solution the output of the other generators would be adjusted as normal to satisfy the area interchange constraints. An example in which changing the actual output might not be appropriate would be a generator with a temperature limit model that is not operating above its limit.

Most of these examples demonstrate results using 1949 weather. There are two reasons for this. First, 1949 is the year of record cold for much of Central

Texas, so it is a good year for comparison with Winter Storm Uri. Second, being more than 70 years ago, it demonstrates that fairly good analysis can be done even using such data and hence all subsequent years could be considered as well. It is important to emphasize that the point of using historical data is not to represent the grid itself at some point in the past. Rather, it is to apply to the grid being studied (usually representing either present day or future conditions) past weather, which since this past weather has already occurred, there is at least some probability of something similar occurring in the future. As previously noted forecasted future conditions could also be used.

As a first example consider the 6700 bus grid from Figure 6 that has 153 WTGs and 36 solar PVs, all of which have been modeled using the paper's approach of weather dependent maximum real limits. The challenge is to set these maximum limits consistently. Of course one approach would be to just study the situations of either full available capacity, or zero available capacity everywhere. While this simplifies the problem, it is likely an over simplification since these two points might not actually represent the most severe operating conditions, and could be quite rare. The challenge for any other operating point is to have a consistent set of limits since the WTG values are correlated by the underlying winds and the solar PVs by their insolation. The solution proposed here is to explicitly include the weather, which if based on observations or meteorological models, provides the correlations.

To determine interesting weather conditions one approach is to quickly process all the weather in a data set by just applying the models to the power flow data without actually solving the power flow. Figure 10 shows the results for the hourly wind and solar generation in the 6700 bus case using the 1949 weather values. Computationally this is relatively quick, scaling with the number of generators and number of time points considered. Even using not particularly optimized code, processing only took about one second per day with hourly data for the 82K bus system. This data at each hour can then be used to determine a power flow or OPF solution (demonstrated with the 24K bus grid).

From this data, interesting conditions can be determined for further study. For 1949 one such time is the record cold that occurred on January 31 (i.e., Figure 1). Figure 11 uses a gray color mapping to visualize the wind generation that occurred at 4 a.m. on 1/31/49 using the same GDV size scale and colors as from Figure 6 (for clarity the non-renewable generation has been removed and obviously there would be no solar at 4 a.m.). Interestingly there was relatively little wind throughout Texas with almost no wind in South Texas; at this time the available wind capacity would be 7.3 GW (out of a total of 25 GW).

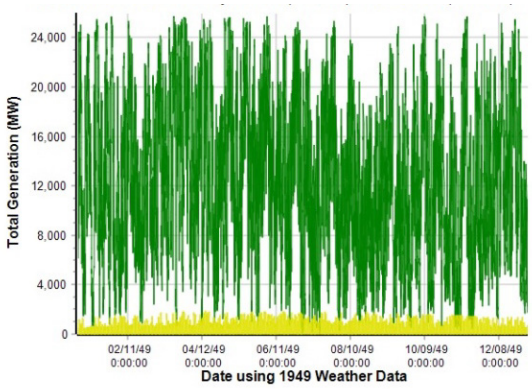

Figure 10: 6700-Bus (2019) Grid Hourly Wind and Solar Capacity using 1949 Data

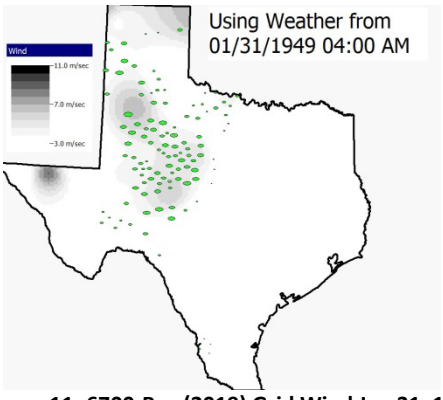

Figure 11: 6700-Bus (2019) Grid Wind Jan 31, 1949

In applying the temperature model to all the natural gas generators, WPPs and solar PV generators using the model's default parameters it appears that there might have been more generation lost compared to Uri if the 1949 weather had occurred. This is because while the temperatures in parts of Texas were higher in 1949, they were lower over the parts of the state with the most natural gas generation. Also, because of the lower winds overall, the WPP outputs would likely have been lower.

Of course, the purpose in this paper is just to introduce the weather inclusion methodology, and not to provide in-depth results for any particular events. But this methodology could be used to provide such results in more detailed studies. Other interesting times can be when there are sudden changes (particularly decreases) in the wind and/or insolation since this can result in a potentially rapid drop in the renewable generation. The largest hourly decrease was 12.9 GW on November 12th at 6 p.m. Figure 12 shows similar results for the 2030 grid.

Moving on to the 24K grid, the explicit representation of weather is likewise helpful particularly since the grid has more than 600 WTGs and more than 600 of mostly small solar PVs. Using the previous approach the renewable capacity at each time point can quickly be determined. The impact of these assumptions on the OPF solution is illustrated in Figure 13 and Figure 14 in which each figure uses GDVs to show the solution generator outputs and a color contour to visualize the bus locational marginal costs (LMPs). Both figures model a near peak load, something that would usually occur in the later afternoon during the summer. However, the first figure, based on the case study of [38], makes the unrealistic assumption of near maximum wind availability. The second figure makes the more realistic assumption of much lower wind, basing the results on (somewhat arbitrarily) July 15, 1949 at 6 p.m. Certainly there can be convergence issues associated with simultaneously changing many power system maximum generator power limits. The key takeaway in this paper is to provide a relatively simple and flexible methodology for explicitly representing the weather to set these limits.

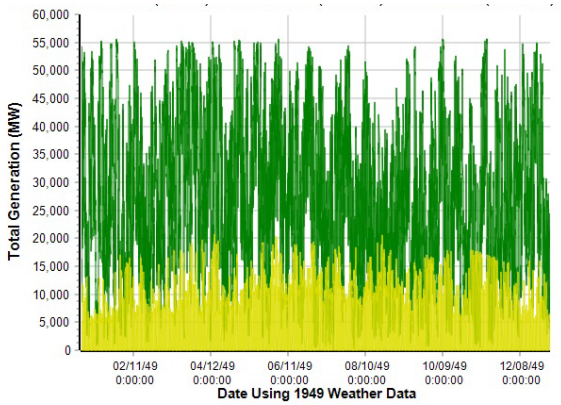

Figure 12: 6700-Bus (2030) Grid Hourly Wind and Solar Capacity using 1949 Data

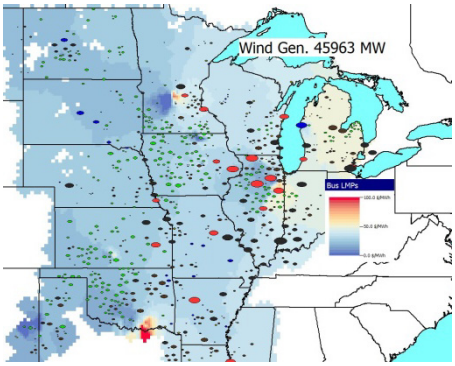

Figure 13: 24K-Bus Grid LMP Contour with High Wind

The last example is with the 82K-bus grid, with this grid included to demonstrate that the approach can be applied to quite large systems. As with the previous examples the system was first screened using the 1949 data, with the hourly renewable generation values shown in Figure 15. With this grid the largest hourly decrease in aggregate was just 3.7 GW, though there was substantially more volatility on a percentage basis in the individual area values. Figure 16 shows the renewable generator values for the hour with the highest values; a gray-scale is used in the figure to show the associated wind speeds.

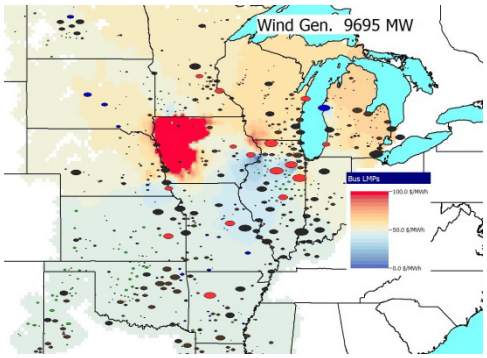

Figure 14: 24K-Bus Grid LMP Contour with Lower Winds

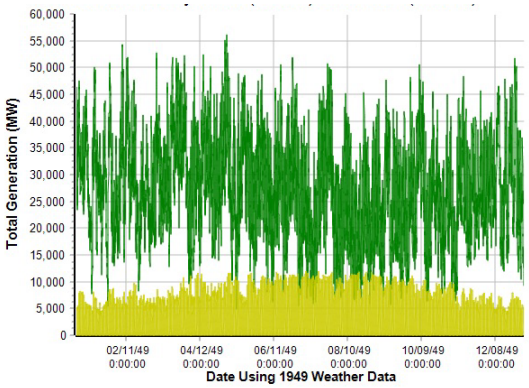

Figure 15: 82K-Bus Grid Hourly Wind and Solar Capacity using 1949 Data

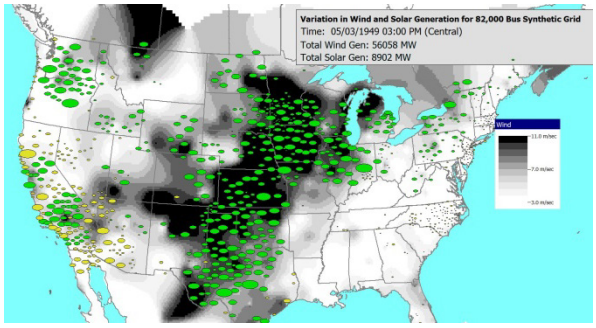

Figure 16: 82K-Bus Grid Renewal Generation using May 3, 1949 Data

As noted in Section 1, there are always tradeoffs associated with engineering modeling. This will certainly be the case with the direct inclusion of weather and weather-related models into the power flow. For example, balancing the number of different models, the complexity of each model, the availability of the model parameters, and the impact of the model outputs on the results. As is the case with electric grid stability analysis, how these issues are addressed will gradually change over time based on results from research and other studies.

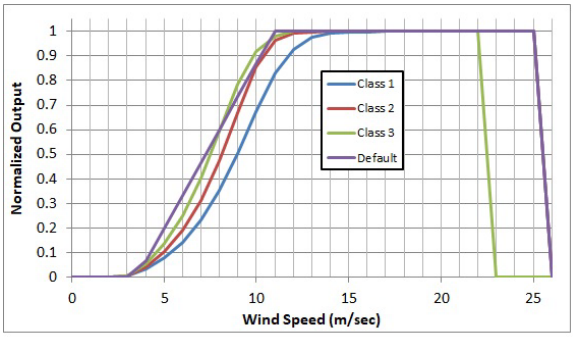

Figure 17: Speed-Power Curves for Different WPP Models

As a step in this direction, Figure 17 shows the curves for the four WPP types modeled here, with the Class 1 to 3 values coming from [33]. While detailed information about all the WPPs in the US is given in [21] (including the specific wind turbine model and hub height), initially it is quite likely that studies would be done using default models. Hence the results presented here have used the simple Default model shown in Figure 17.

To look at the sensitivity of the results to this assumption, Figure 18 compares the wind results from Figure 15 with the results that are obtained using the assumption of all Class 1 models (i.e., WPPs designed for high wind conditions). The average difference is about 6500 MW. Since the Class 1 model is the most different from the Default and represents a very small percentage of the WPPs in the US (most are Class 2), this difference over estimates what would be obtained if detailed models had been used for all the WPPs.

Of course what degree of detail is needed and how errors from one assumption compare with others is study specific. To give a final example that briefly considers how the models can be validated and improved, on July 11, 2022 the Electric Reliability Council of Texas (ERCOT) had an extremely high electric load due to hot conditions across their footprint and low wind generation. As noted in [39] ERCOT had installed wind and solar capacity of 35.1 GW and 11.8 GW respectively. In order to compare the paper's synthetic 6700 bus grid results with the actual conditions from this day, the synthetic grid's generation, which was originally based on 2019 data, was augmented to match the size and location of the actual July 2022 wind and solar capacity in ERCOT. Since the specific details on the wind class was not in the synthetic grid, as a simplification all the wind generation was assumed to be Class 2. Weather data for July 11, 2022 at 3 p.m. (CDT) was obtained from [13], and then the algorithm was applied to determine the estimated wind generation. Since default models were used and the weather data was readily available, this took very little additional work to include this weather dependence in the power flow.

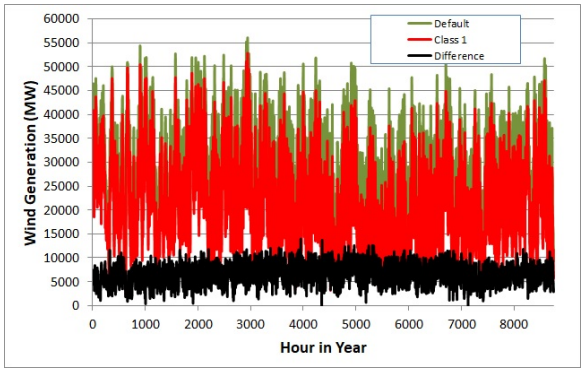

Figure 18: Difference in 82K-Bus Hourly Winds between Using the Default Model and the Class 1 Model

Depending on the assumed hub height scalar the estimated wind generation ranged from 3815 MW for a scalar of 1.2 to 5970 MW for a scalar of 1.4. This compares favorably to the actual value reported by ERCOT of about 3700 MW (with the value rapidly varying from 2000 MW at 2 p.m. to 5400 MW at 4 p.m.). Figure 19 shows a contour of the wind at 3 p.m. using the Figure 16 color mapping along with the assumed outputs of the 6700 bus grid wind (green) and solar (yellow) generators; the dots show the location of the weather measurements obtained from [13].

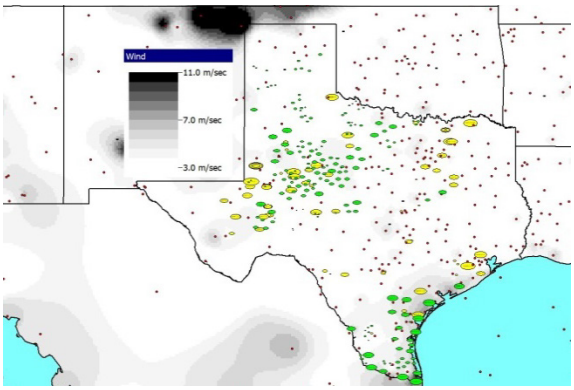

Figure 19: July 11, 2022 Wind Contour at 3 p.m. CDT

Figure 20 shows a zoomed view of this same data, except with the values of the actual wind measurements shown in the white boxes and the WTG outputs shown in the green ovals. Note that over relatively small distances the wind speed can vary substantially (e.g., from 3 m/s to 10 m/s). Hence as was the case from earlier of the Columbia River Gorge, the results could likely be improved substantially by ensuring that the appropriate wind measurements, WTG model classes, and hub height scalar are assigned to the WTGs in this region. Of course whether this level of detail is needed would be study specific, but once these modeling details have been determined, they could be used in all future studies.

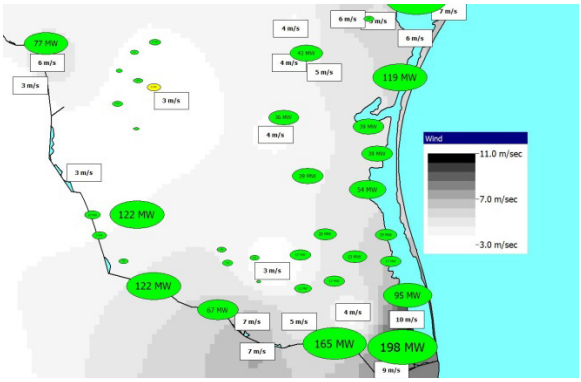

Figure 20: July 11, 2022 Wind Contour at 3 p.m. CDT, Zoomed View of South Texas

5. Conclusion and Future Directions

The paper has shown that it is fairly straightforward to explicitly include weather data in power flow models and that there are significant advantages associated with this approach. The issues that have been addressed include the availability of weather data, the mapping of weather information to electric grid components, and the development of a flexible and extensible modeling approach for relating weather values to the power flow models. Several large-scale examples have been presented with consideration of the visualization of the results. There are many directions for future work including the development of many more models, the sensitivity of the results to the models, computational considerations in processing many different time periods, and power flow convergence issues in moving between different time points.

6. Acknowledgements

This work was partially supported through funding provided by the US ARPA-E, the Power Systems Engineering Research Center (PSERC), and the Texas A&M Smart Grid Center.

6. References

[1] J.B. Ward, H.W. Hale, "Digital Computer Solution of Power Flow Problems," *AIEE Transactions*, vol. 75, pp. 394-404, June 1956.

[2] W.F. Tinney, C.E. Hart, "Power Flow Solution by Newton's Method, *IEEE Trans. Power App. & Syst*., vol. pas-86, pp. 1449-1460, Nov. 1967.

[3] "Common Format for Exchange of Solved Load Flow Data," *IEEE Trans. Power App. & Syst*., vol. pas-92, pp. 1916-1925, Nov/Dec 1973.

[4] "NERC Library of Standardized Power Flow Parameters and Standardized Dynamic Models, Version 1.0," North American Electric Reliability Corporation, Atlanta, GA, Oct. 2015.

[5] "WECC Data Preparation Manual for Interconnection-Wide Cases," WECC, Salt Lake City, UT, 2019.

[6] J. Yeo, P. Dehghanian, and T. J. Overbye, "Power flow consideration of impedance correction for phase shifting transformers," IEEE Texas Power and Energy Conference (TPEC), College Station, TX, Feb. 2019.

[7] J. Arrillaga, C.P. Arnold, *Computer Analysis of Power Systems*, John Wiley & Sons, Chichester, UK, 1990 (Chapter 3, Three-Phase Load Flow)

[8] A.J. Wood, B.F. Wollenberg, *Power Generation, Operation and Control*, 2nd edition, John Wiley & Sons, New York, NY, 1996.

[9] *The February 2021 Cold Weather Outages in Texas and the South Central United States*, U.S. Federal Energy Regulatory Agency (FERC), Nov. 2021.

[10] Enhancing the Resilience of the Nation's Electricity System, The National Academies Press, Washington, DC, 2017

[11] A. Bose, T. J. Overbye "*Electricity Transmission System Research and Development: Grid Operations*," In Transmission Innovation Symposium: Modernizing the U.S. Electrical Grid, U.S. Department of Energy 2021.

[12] Data from *Weather Graphics* at www.weathergraphics.com/identifiers/

[13] Current Weather and Wind Station Data, https://aviationweather.gov/adds/dataserver_current/current/metars.cache.csv (accessed May 29, 2022)

[14] T. J. Overbye, E. M. Rantanen and S. Judd, "*Electric power control center visualization using Geographic Data Views,*" 2007 iREP Symposium – Bulk Power System Dynamics and Control – VII. Revitalizing Operational Reliability, Charleston, SC, August, 2007.

[15] TPL-007-4, "Transmission System Planned Performance for Geomagnetic Disturbance Events," NERC, Atlanta, GA, October 2020.

[16] Southwest Power Pool (SPP) Model Development Procedure Manual, Version 4.0, SPP, July 2020.

[17] MISO Reliability Planning Model Data Requirements and Reporting Procedures, Version 4.0, MISO, August 2021.

[18] A.B. Birchfield, K.M. Gegner, T. Xu, K.S. Shetye, and T.J. Overbye, "Statistical Considerations in the Creation of Realistic Synthetic Power Grids for Geomagnetic Disturbance Studies," IEEE Transactions on Power Systems, vol. 32, pp. 1502-1510, Mar. 2017

[19] F. Safdarian, A. Birchfield, K. Shetye, and T.J. Overbye, "Additional Insights in Creating Large-Scale, High-Quality Synthetic Grids: A Case Study," Kansas Power and Energy Conference (KPEC), Apr. 2021.

[20] Texas A&M University Electric Grid Test Case Repository, electricgrids.engr.tamu.edu.

[21] U.S. Energy Information Association Form EIA-860, 2021; www.eia.gov/electricity/data/eia860

[22] T.J. Overbye, K. Shetye, J. Wert, H. Li, C. Cathey, H. Scribner, "Stability Considerations for a Synchronous Interconnection of the North American Eastern and Western Electric Grids," Proc. 55th Hawaii International Conference on System Sciences (HICSS), Jan. 2022

[23] J. Sharp, C. F. Mass, "Columbia Gorge Gap Winds: Their Climatological Influence and Synoptic Evolution," Weather and Forecasting, vol. 19, pp. 970-992, 2004.

[24] M. S. Dyrkacz, C. C. Young, and F. J. Maginniss, "A digital transient stability program including the effects of regulator, exciter, and governor response," *AIEE Trans. (Power App. & Syst.)*, vol. 79, pp. 1245-1257, Feb. 1961.

[25] IEEE Committee Report, "Computer representation of excitation systems," IEEE Trans. Power App. & Syst, vol. PAS-87, pp. 1460–1464, June 1968.

[26] IEEE Std 421.5-2016, IEEE Recommended Practice for Excitation System Models for Power System Stability Studies, IEEE, 2016.

[27] U.S. Federal Energy Regulatory Commission (FERC) Order 881, December, 2021; online at www.ferc.gov/media/e-1-rm20-16-000

[28] S. Tandon, S. Grijalva, D.K. Molzanh, "Motivating the User of Dynamic Line Ratings to Mitigate the Risk of Wildfire Ignition," 2021 Power and Energy Conference at Illinois, Urbana, IL, April 2021.

[29] A. Ahmed, F. J. Stevens McFadden, R. Rayudu, "Weather-Dependent Power Flow Algorithm for Accurate Power System Analysis Under Variable Weather Conditions," IEEE Trans. Power Systems, vol. 34, pp. 2719-2729, July 2019.

[30] G. M. Masters, *Renewable and Efficient Electric Power Systems*, 2nd Edition, IEEE Press, 2013.

[31] V. Sohoni, S.C. Gupta, R.K. Nema, "A Critical Review on Wind Turbine Power Curve Modelling Techniques and Their Applications in Wind Based Energy Systems," *Journal of Energy*, vol. 2016, dx.doi.org/10.1155/2016/8519785

[32] P. Giorsetto, K.F. Utsurogi, "Development of a New Procedure for Reliability Modeling of Wind Turbine Generators," *IEEE Trans. Power App. & Syst.*, vol. PAS-102, pp. 134-143, Jan. 1983.

[33] C. Draxl, A. Clifton, B. Hodge, J. McCaa, "The Wind Integration National Dataset (WIND) Toolkit," Applied Energy, vol. 151, pp. 355-366, 2015.

[34] A. De Sa., S. A. Zubaidy, "Gas Turbine performance at varying ambient temperature," *Applied Thermal Engineering*, vol. 31, pp. 2735-2739, 2011.

[35] S. Murphy, F. Sowell, J. Apt, "A time-dependent model of generator failures and recoveries captures correlated events and quantifies temperature dependence," *Applied Energy*, vol. 253, 2019.

[36] A.B. Birchfield, T. Xu, K. Gegner, K.S. Shetye, and T.J. Overbye, "Grid Structural Characteristics as Validation Criteria for Synthetic Networks," IEEE Transactions on Power Systems, vol. 32(4), pp. 3258-3265, Jul. 2017.

[37] Texas A&M University Electric Grid Datasets, electricgrids.engr.tamu.edu.

[38] J.L. Wert, F. Safdarian, T.J. Overbye, D.J. Morrow, "Case Study on Design Considerations for Wide-Area Transmission Grid Operation Visual Storytelling," 2022 Kansas Power and Energy Conference, Manhattan, KS, May 2022.

[39] ERCOT July 10, 2022 News Release, www.ercot.com/news/release?id=90030206-5cf5-db8e-13d1-f8fe2bd0128f